Provided for non-commercial research and education use.
Not for reproduction, distribution or commercial use.

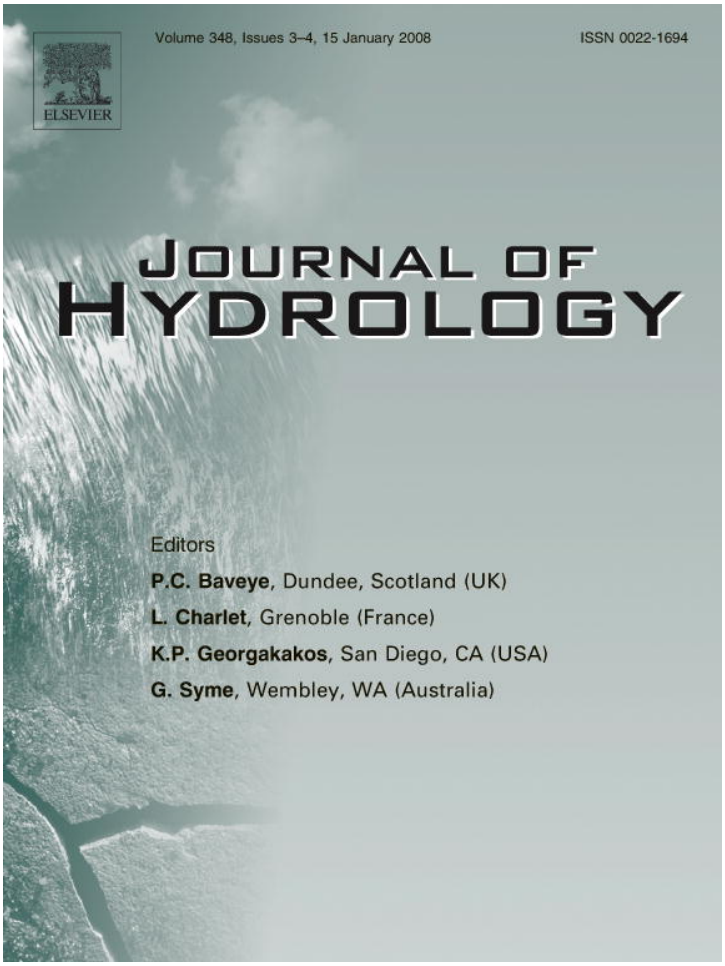

This article was published in an Elsevier journal. The attached copy is furnished to the author for non-commercial research and education use, including for instruction at the author's institution, sharing with colleagues and providing to institution administration.

Other uses, including reproduction and distribution, or selling or licensing copies, or posting to personal, institutional or third party websites are prohibited.

In most cases authors are permitted to post their version of the article (e.g. in Word or Tex form) to their personal website or institutional repository. Authors requiring further information regarding Elsevier's archiving and manuscript policies are encouraged to visit:

http://www.elsevier.com/copyright

Author's personal copy

Journal of Hydrology (2008) **348**, 395–411

available at www.sciencedirect.com

ScienceDirect

journal homepage: www.elsevier.com/locate/jhydrol

Two-scale modeling of solute transport in an experimental stratigraphy

Ye Zhang [a,*], **Carl W. Gable** [b]

[a] *Department of Geological Sciences, University of Michigan, 2534 CC Little Bldg, Ann Arbor, MI 48109, United States*
[b] *EEES-6, Los Alamos National Laboratory, Los Alamos, NM 87545, United States*

Received 7 April 2007; received in revised form 24 September 2007; accepted 10 October 2007

KEYWORDS
Experimental stratigraphy;
Hydraulic conductivity;
Heterogeneity;
Solute transport;
Anomalous dispersion;
Macrodispersion

Summary A high-resolution non-stationary hydraulic conductivity map is generated based on an experimental stratigraphy. A heterogenous model is created, incorporating the complete conductivity variation. A hydrostratigraphic model (HSM) is also created which divides the space into discrete lithofacies units. For each unit, an equivalent conductivity is estimated using numerical up-scaling. Under a lateral hydraulic gradient, steady-state, incompressible groundwater flow experiments are conducted in both models. Within each flow field, conservative pulse-input line-source tracer is simulated. In the heterogeneous model, the tracer exhibits both scale-dependency in the observed longitudinal macrodispersivity and persistent long tailing associated with anomalous, non-Fickian dispersion. In comparison, HSM-predicted, global mean relative error of hydraulic head is 1.5%, that of groundwater flux is 0.77%. Using (small) hydrodynamic dispersivities, the HSM closely predicts the evolution of the tracer moments. A certain degree of tailing is also predicted, as this model has captured the largest scale, between-unit velocity variations. However, detailed plume shape is not captured, nor are the arrival and tailing of the breakthrough curves. Using macrodispersivity (both unit-specific and time-dependent), the breakthrough prediction has improved, especially the solute arrival time. Both macrodispersion models also capture the development of breakthrough asymmetry as well as power-law tailing. However, the development of a steep front and multiple peak concentrations are not captured. Similar observations are also found for a continuous-source injection. Overall, for the chosen boundary condition, the advection–dispersion equation can be used by the lithofacies model to capture certain key aspects of the bulk flow and transport behaviors, although displacement mapping reveals that heterogeneity-induced dispersion is correlated both in time and space, a likely result of the correlated velocity field.
© 2007 Elsevier B.V. All rights reserved.

* Corresponding author. Present address. Department of Geology and Geophysics, University of Wyoming, 1000 University Ave, Laramie, WY 82071, United States.
E-mail addresses: ylzhang@umich.edu, yzhang9@uwyo.edu (Y. Zhang).

0022-1694/$ - see front matter © 2007 Elsevier B.V. All rights reserved.
doi:10.1016/j.jhydrol.2007.10.017

Author's personal copy

Introduction

Hydraulic conductivity (K) heterogeneity, which exists at all scales in natural porous media, is a critical factor influencing solute migration. Because of such importance, in numerical flow and transport studies, some level of heterogeneity is often incorporated into the models. However, most models do not account for heterogeneity at all scales, due to lack of data and/or computation limit. For example, heterogeneity is sometimes populated throughout the solution domain, i.e., each numerical cell is given a grid conductivity/dispersivity which account for flow/transport behaviors arising out of the unresolved sub-grid heterogeneities (e.g., Efendiev et al., 2000; Rubin et al., 2003; Fernàndez-Garcia and Gómez-Hernández, 2007). At larger scales where multiple aquifers exist, heterogeneity is often represented by a series of internally homogeneous units, e.g., facies mapping can identify zones of relative homogeneity. At regional to basin scales, such units can correspond to geological formations. This second type of heterogeneity characterization is geology based, and is referred to herein as a hydrostratigraphic model (HSM). This study is concerned with this type of model.

To quantify groundwater flow using HSM, a representative conductivity is assigned to each unit to relate the mean head gradient to the average groundwater fluxes. To quantify solute transport, a field-scale dispersivity or macrodispersivity is used to represent solute spreading due to the unresolved, within-unit heterogeneity. Specifically, using velocities obtained by solving the groundwater flow equation, the advection–dispersion equation (ADE) is solved for solute concentrations. While representative conductivity may be obtained using up-scaling methods (e.g., Renard and de Marsily, 1997; Sanchez-Vila et al., 2006), the estimation of macrodispersivity is much less certain. Compared to hydrodynamic dispersion observed in laboratory column studies, macrodispersion is attributed to velocity variations at scales larger than the scale of continuum flow representation (i.e., the Darcy scale), but smaller than the scale of explicit model characterization (i.e., a hydrogeologic unit). In practice, macrodispersivity is often assumed constant in space, e.g., an adjustable parameter of a model unit. Alternatively, time-dependent macrodispersivity has been used. Though such practice underlies model evaluation of a variety of hydrogeological problems, macrodispersivity estimated from field and modeling studies is found to increase as the scale of observation increases (Gelhar et al., 1992). This ''scale effect'' is often attributed to solute channeling through preferential flow paths, though using ADE with localized parameters to interpret breakthrough (while ignoring the underlying transport complexity) can certainly also contribute. The applicability of the macrodispersion model (ADE + macrodispersivity) also depends on solute body dimensions: it may work well (in a stationary medium) if the plume size is large compared to the scale of heterogeneity. These issues call into question the uniqueness of macrodispersivity assigned to the model unit and, the applicability of ADE to represent transport in heterogeneous media.

Perturbation-based stochastic theories have been developed to estimate (ensemble) macrodispersivities for heterogeneous media based on geostatistical parameters of small-scale conductivity (Dagan, 1989; Gelhar, 1993; Dagan and Neuman, 1997; Rubin, 2003). Simplifying assumptions are often adopted, e.g., stationarity, weak heterogeneity (variance of $\ln K < 1$), large problem scale (compared to $\ln K$ correlation range). However, conductivity of natural deposit is often non-stationary at multiple scales or exhibits complex trends that defy simple statistical description. It can also exhibit long-range correlation, e.g., preferential flow paths or barriers. In such cases, solute transport often does not reach the Fickian state for which the classic results are applicable (thus the term ''anomalous transport''). To describe transport in such media, alternative theories are proposed, based on either variations of ADE (e.g., Haggerty and Gorelick, 1995; Harvey and Gorelick, 2000; Benson et al., 2000) or non-local formulations that do not invoke the Fickian assumption (e.g., Zhang and Neuman, 1990; Wheatcraft and Cushman, 1991; Zhang, 1992; Cushman and Ginn, 1993; Glimm et al., 1993; Neuman, 1997; Guadagnini and Neuman, 2001; Morales-Casique et al., 2006). Based on continuous time random walk, non-perturbative theories are also developed which has shown promise in representing transport in multiscale media (Berkowitz et al., 2002; Cortis et al., 2004). However, alternative approaches often involve numerical convolution or require mapping of the fine-scale behavior onto the up-scaled model via, e.g., parameter fitting of observed breakthrough.

Parallel to the conceptual development is the recognition that natural heterogeneity is dominated by sedimentary structures (e.g. Fogg, 1990; Scheibe and Freyberg, 1995; Anderson, 1997; Webb and Davis, 1998; LaBolle and Fogg, 2001). By combining geologic information with analysis of small-scale heterogeneity, multiscale conductivity has been explicitly modelled (e.g. Jussel et al., 1994; Webb and Anderson, 1996; Tompson et al., 1998; Bersezio et al., 1999; Lu et al., 2002; Weissmann et al., 2002; Zhou et al., 2003). Assumptions concerning heterogeneity are usually made, resulting in significant uncertainties in the predicted conductivity structure. Since geological ''ground-truth'' is rarely known, it is generally difficult to determine the relative merits of ADE versus alternative approaches in modeling transport. For example, at a given discretization, the dual-domain model was able to predict field-scale spreading more accurately (Feehley et al., 2000). However, ADE may improve if a more resolved characterization is possible, thus the general recommendation that heterogeneity be resolved at as small scale as possible. However, work by Eggleston and Rojstaczer (1998) highlights the difficulty in understanding local conductivity variation, even with exhaustive sampling.

In this study, the recognition that multiscale heterogeneity exists on the one hand, and the practical need to construct transport simulators which rely on hydrogeologic units, representative conductivity, and macrodispersivity on the other (e.g. Zhang et al., 2005a), motivates an analysis based on a high-resolution, fully heterogeneous hydraulic conductivity map, created from an experimental stratigraphy (Zhang et al., 2005b). The conductivity map is unique compared to other synthetic data: the heterogeneity pattern corresponds to physical sedimentation that is statistically inhomogeneous. It is multiscale, exhibiting both global sand/clay transitions and local-scale variations unique to the depositional processes. Many regions of the

Author's personal copy

map exhibit long-range stratifications (connected preferential flow paths) and/or complex spatial trends. Since small-scale heterogeneity can significantly impact transport, such spatial features need to be fully resolved. By discretizing the map down to the scale of each pixel, a high-density finite element grid (424,217 nodes and 845,208 elements; details on grid generation can be found in Zhang et al., 2006) is created for which a heterogeneous model completely incorporates the conductivity variation (Fig. 1a). A hydrostratigraphic model (HSM) is then created based on the observed lithofacies discontinuities which divide the map into 14 non-overlapping units (Fig. 1b). The full map *lnK* variance is 4.07, reflecting an unconsolidated alluvial fan; that of the HSM units ranges from 0.31 to 1.85 (Table 1), comparable to many natural aquifers (Hoeksema and Kitanidis, 1985; Anderson, 1997).

This study is an extension of earlier studies in which detailed discussions on map creation can be found. For representative subregions, Zhang et al. (2005b) calculates the experimental ln*K* variograms and estimates the (anisotropic) integral scales. For the HSM, Zhang et al. (2006) computes an equivalent conductivity ($\mathbf{K}^*$) for each unit via up-scaling. By comparing flow and transport predictions of the heterogeneous model and the up-scaled model, the impact of unresolved heterogeneity can be assessed. In Zhang et al. (2006), hydraulic head, flow paths and groundwater fluxes are evaluated in a basin-scale setting. In this study, the conductivity map is re-scaled to 100 m long and ~8 m thick (Fig. 1a); each local conductivity corresponds to a REV of $0.1 \times 0.02\ m^2$, or approximately core scale. Solute transport is evaluated deterministically: in the heterogenous model, the ADE is assumed applicable; in the HSM, the same ADE is solved using macrodispersivities to represent solute spreading due to the unresolved, within-unit heterogeneity. Note that though many alternative approaches are developed in recent literature to model transport in non-stationary media, this study evaluates the classic (Gaussian-based) macrodispersion theory first. Several reasons exist for this decision: (1) this theory is the most widely studied and has matured to an extent that its underlying assumptions are generally well understood (Rubin, 2003); (2) most

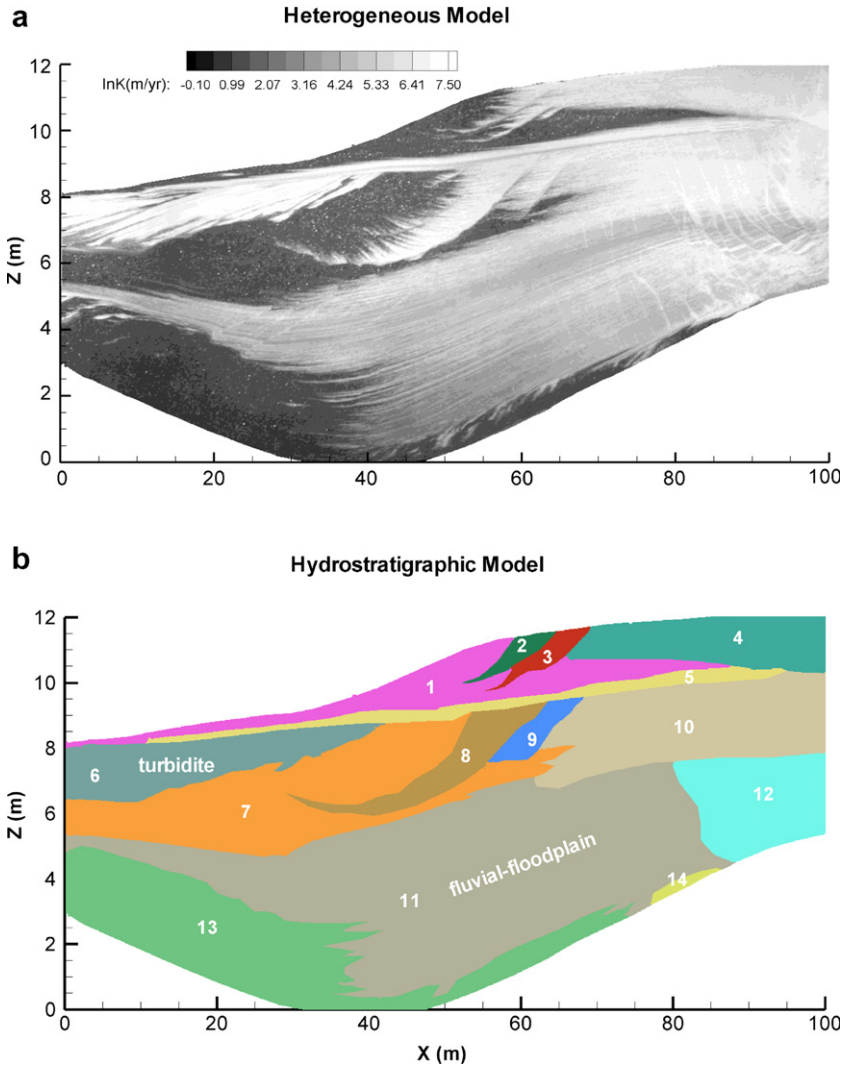

Figure 1 (a) Conductivity of the heterogeneous model, plotted in natural log scale; (b) Unit tag of the hydrostratigraphic model. Note the location of a turbidite unit and a fluvial-floodplain unit.

Author's personal copy

Table 1 Equivalent conductivity (m/y) estimated for the HSM units, along with the ln*K* variance, integral scales (m) and longitudinal macrodispersivity (m) predicted by a stochastic theory

Unit ID	K_{xx}	K_{zz}	K_{xz}	σ_f^2	λ_{max}	λ_{min}	α_L^M
1	17.13	7.09	0.22	0.73	0.13	0.03	0.09
2	163.06	75.98	−15.14	1.48	1.00	0.04	1.48
3	290.02	105.37	−8.85	1.15	1.00	0.04	1.15
4	328.83	258.12	0.52	0.31	0.52	0.03	0.16
5	582.83	223.45	−11.20	0.91	0.52	0.03	0.47
6	828.28	163.23	15.84	1.85	4.35	0.05	8.06
7	14.53	7.15	−0.20	0.83	0.13	0.03	0.10
8	499.54	259.20	108.81	1.25	2.05	0.04	2.57
9	304.40	142.52	−1.60	1.13	2.05	0.04	2.33
10	571.38	542.98	8.78	0.37	0.45	0.05	0.17
11	128.73	70.21	0.66	1.10	1.50	0.03	1.65
12	370.30	220.73	−1.55	0.62	0.88	0.08	0.54
13	5.07	3.72	0.01	0.41	0.13	0.03	0.05
14	11.29	6.73	0.52	0.59	0.13	0.03	0.07

λ_{max} and λ_{min} are the integral scales along the major and minor statistical axis, respectively, obtained from re-scaling those estimated for the subregions (Zhang et al., 2005b). Due to small bedding angle and the lateral flow condition, λ_{max} approximates λ (integral scale along mean flow direction); λ_{min} approximates vertical integral scale.

numerical studies conducted to evaluate this theory base their conclusions on simplistic heterogeneities (typically, multi-Gaussian lognormal *K* field with stationary isotropic or anisotropic covariance); (3) our previous work has estimated the necessary geostatistical parameters. The simulation framework and associated assumptions used in this study are summarized in Fig. 2.

The goals of this study are threefold: (1) How does macrodispersion play out in this multiscale medium? Will scale effect occur as a result of Fickian assumption? (2) Can the ADE-based up-scaled model capture aspects of the bulk transport behavior? And what aspects? (3) Comparing the two models, what is the nature of heterogeneity-induced dispersion and what is the limitation of the macrodispersion model? In addressing (1), moment analysis is conducted on a tracer simulated by the heterogeneous model. A Fickian-based equation is used to infer a tracer macrodispersivity. In addressing (2), the same tracer is simulated by the HSM, first using hydrodynamic dispersivity then macrodispersivity. Tracer moments and breakthroughs are compared to those of the heterogeneous model. In addressing (3), macrodispersive displacement is mapped over time by comparing solute trajectories predicted by the two models. In the rest of this paper, the flow and transport experiments are first described, followed by 4 sections addressing the above questions. Discussions and conclusions are then presented, followed by future research directions.

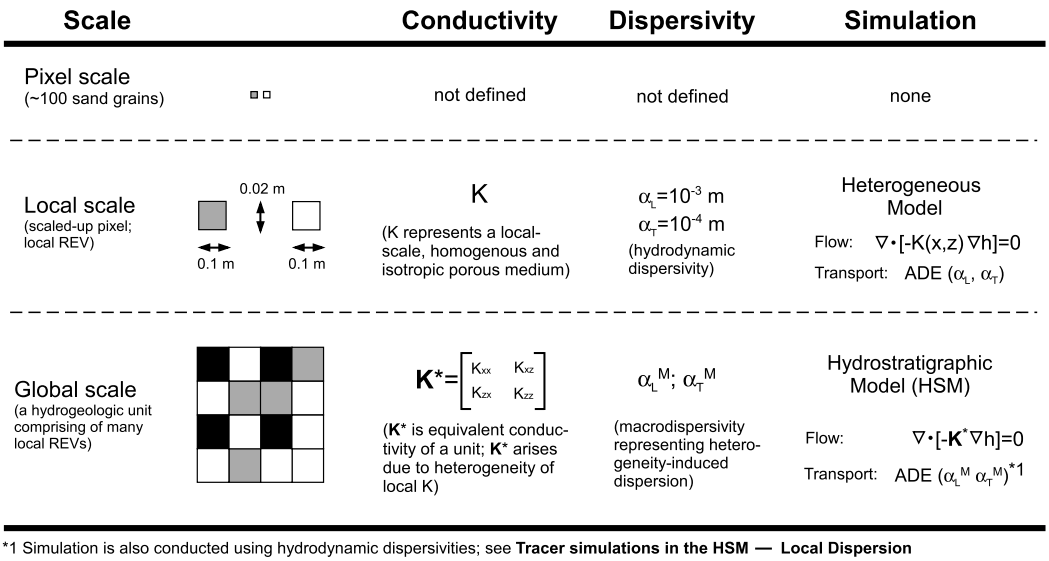

Figure 2 Schematic diagram of the assumptions used by the models. Pixel scale corresponds to the original stratigraphy. All models of flow and transport are conducted at the local and global scales using the same high-density grid.

Author's personal copy

Flow and transport experiments

Conductivity up-scaling

In this study, an up-scaling analysis is first conducted to find the equivalent conductivity ($\mathbf{K}^*$) for each unit of the HSM. The up-scaling is accomplished by conducting steady-state, incompressible flow experiments in the heterogeneous model. To capture the full tensor characteristics of $\mathbf{K}^*$, in each experiment, different boundary condition is assigned to the model periphery. For each unit, $\mathbf{K}^*$ is calculated using the global Darcy's law by incorporating results from all experiments:

$$B.C.1: \begin{Bmatrix} \langle q_x \rangle_1 \\ \langle q_z \rangle_1 \end{Bmatrix} = -\begin{bmatrix} K_{xx} & K_{xz} \\ K_{zx} & K_{zz} \end{bmatrix} \begin{Bmatrix} \langle \partial h/\partial x \rangle_1 \\ \langle \partial h/\partial z \rangle_1 \end{Bmatrix}$$

$$\cdots$$

$$B.C.m: \begin{Bmatrix} \langle q_x \rangle_m \\ \langle q_z \rangle_m \end{Bmatrix} = -\begin{bmatrix} K_{xx} & K_{xz} \\ K_{zx} & K_{zz} \end{bmatrix} \begin{Bmatrix} \langle \partial h/\partial x \rangle_m \\ \langle \partial h/\partial z \rangle_m \end{Bmatrix}$$

$$\begin{bmatrix} \langle \partial h/\partial x \rangle_1 & \langle \partial h/\partial z \rangle_1 & 0 & 0 \\ 0 & 0 & \langle \partial h/\partial x \rangle_1 & \langle \partial h/\partial z \rangle_1 \\ \cdots & \cdots & \cdots & \cdots \\ \langle \partial h/\partial x \rangle_m & \langle \partial h/\partial z \rangle_m & 0 & 0 \\ 0 & 0 & \langle \partial h/\partial x \rangle_m & \langle \partial h/\partial z \rangle_m \end{bmatrix} \begin{Bmatrix} K_{xx} \\ K_{xz} \\ K_{zx} \\ K_{zz} \end{Bmatrix} = -\begin{Bmatrix} \langle q_x \rangle_1 \\ \langle q_z \rangle_1 \\ \cdots \\ \langle q_x \rangle_m \\ \langle q_z \rangle_m \end{Bmatrix} \quad (1)$$

where $\langle\rangle$ represents spatial averaging; q_x, q_z are components of the Darcy flux; K_{xx}, K_{xz}, K_{zz} are components of the equivalent conductivity (symmetry is imposed, i.e., $K_{xz} = K_{zx}$); h is hydraulic head; m is the number of flow experiments ($m \geqslant 2$). In this study, $m = 2$ ($\mathbf{K}^*$ is obtained via exact solution). The relevant boundary conditions of the flow experiments are: (1) vertical mean flow: top and bottom boundaries are specified head; no-flow for the sides; (2) lateral mean flow: top and bottom are no-flow; specified head for the sides. More details on the up-scaling method are described in Zhang et al. (2006). This earlier study also finds that the equivalent conductivity is insensitive to the assignment of boundary condition, most likely because the up-scaling domain (various lithofacies units) is generally large compared to the *lnK* correlation scale of each unit.

In this study, the model domain length-to-thickness ratio is 12.5, 1/4 of the ratio of the previous study. The average bedding angle is slightly larger at 3–4°, suggesting more significant off-diagonal terms. For most HSM units (Fig. 1b), the computed equivalent conductivities are diagonally dominant full tensors (Table 1). They differ from those of the previous study: on average, K_{xx} is 6.5% smaller, K_{zz} is 5.4% larger, and the magnitude of K_{xz} is 4.4 times larger, as expected. These conductivities are assigned to the HSM units in the subsequent flow simulation.

Flow simulations

A steady-state, incompressible groundwater flow equation is solved by both the heterogeneous model and the HSM. The top and bottom boundaries are no-flow. The left side is assigned a constant head of 1.0 m; the right side 2.0 m. A lateral head gradient is 1%. As in the previous study, the only difference between models is local conductivity assignment: K of the heterogeneous model versus the full tensor $\mathbf{K}^*$ of the HSM. Boundary condition, grid, and numerical solver remain the same. The boundary condition is chosen because it is comparable to natural settings and other heterogeneity-related studies. The velocity field also directly maps the underlying heterogeneity. Compared to other boundary conditions, e.g., topography-driven flow (Zhang et al., 2006), the HSM-predicted flow paths exhibit less deviations from those of the heterogeneous model.

An absolute head deviation can be defined: $\Delta h = h_{\mathrm{HSM}} - h_{\mathrm{ref}}$, h_{HSM} and h_{ref} are the nodal head computed by the HSM and the heterogeneous (or reference) model, respectively. Δh is contoured in the domain, superimposed onto the conductivity map of the HSM (Fig. 3a). The conductivity (i.e., K_{xx}) is smooth, reflecting the major stratigraphic division. A mean error is defined as: $\mathrm{ME} = \frac{1}{n}\sum_{i=1}^{n}|\Delta h|$, where n is the number of grid nodes (424, 217). The ME normalized by the absolute head drop is 1.5%, close to that of Experiment 2 in the previous study (obtained with the same two sets of boundary condition). The overall Δh characteristics are also similar, i.e., location of head over- and under-estimation (see Fig. 10 in Zhang et al., 2006). Detailed pattern of Δh has changed, however, suggesting the sensitivity of prediction error to changing domain aspect ratio.

Groundwater velocity is computed, assuming a constant porosity of 0.25. Since the end-member conductivities used to create the map are those of unconsolidated sand and clay (Zhang et al., 2005b), such an assumption is considered reasonable. Comparing the velocity magnitude ($v = |\vec{v}|$) of both models (Figs. 3b & c and 4a & b), the heterogeneous model exhibits multiscale variability with near identical pattern to the underlying ln$K$ map. That computed by the HSM captures the largest scale, between-unit velocity variations, i.e., among the sand-rich and clay-rich units. Due to homogenization, it is smooth within each unit, as expected. Moreover, deviation in v ($\Delta v = v_{\mathrm{HSM}} - v_{\mathrm{ref}}$) directly maps the unresolved, within-unit heterogeneity (Fig. 4c). Viewed against the heterogeneity map, negative deviation is observed in high-K deposit, positive deviation in low-K deposit, as expected.

Along the recharge and discharge boundaries, total integrated fluxes (Q) are also computed (Fig. 3b & c). The HSM underestimates that of the heterogeneous model by ~0.77%. Overall, for the chosen boundary condition, the HSM has captured the bulk flow characteristics of the heterogeneous model, but not the detailed (within-unit) velocity variations.

Transport simulations

Within the velocity fields computed by both models, conservative solute transport is simulated to represent an instant line-source release. To avoid numerical dispersion and oscillation in solving transport in highly detailed heterogeneity, random walk particle tracking (RWPT) is used. A particle tracking program is developed for finite element grids with arbitrary configuration. It is verified by generating correct analytic flow paths (Zhang, 2005). RWPT is not error-proof,

Author's personal copy

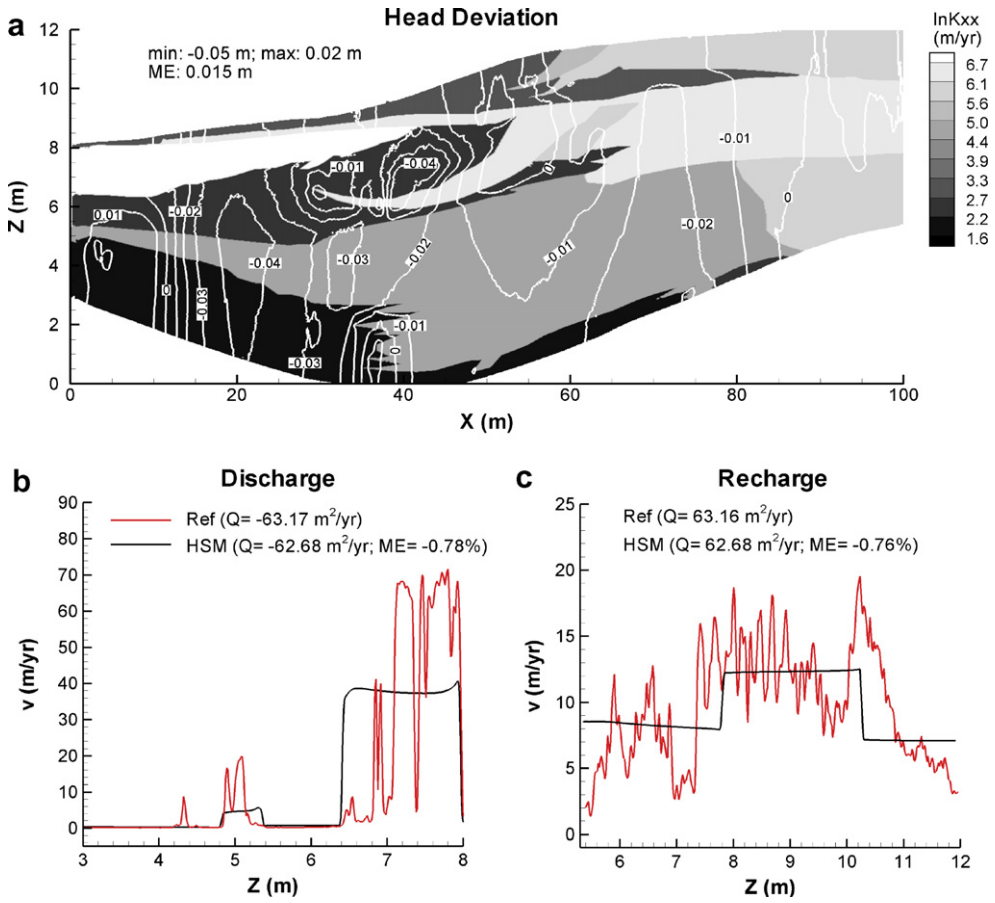

Figure 3 (a) Head deviation (Δh; m) of the HSM superimposed onto the conductivity map. The minimum and maximum Δh are shown, along with a ME. Magnitude of the groundwater velocity is computed along the discharge (b) and recharge (c) boundaries. For each model, total recharge and discharge fluxes (Q) are also computed along the same boundaries. A mean relative error is defined as: $\mathrm{ME}(\%) = (|Q_{\mathrm{HSM}}| - |Q_{\mathrm{ref}}|)/|Q_{\mathrm{ref}}| \times 100$.

however, as local mass balance error can become significant when conductivity contrast is large (LaBolle et al., 1996). In this study, heterogeneity is relatively smooth-varying, such error is not deemed significant.

At initial time, the tracer is simulated near the recharge boundary by randomly generating 10,000 particles within a 5 (vertical) $\times$ 0.1 (horizontal) m^2 zone centered on x = 99.18 m. The initial mass distribution thus reflects uniform concentration. Since conductivity does not vary significantly in the upstream flow field (of both models), flux-weighted scheme is not considered. Tracer vertical dimension samples a large region of the flow field. It is large compared to the vertical ln$K$ integral scale (0.02—0.08 m) (Table 1), satisfying theory requirement of a large plume in direction orthogonal to flow (Quinodoz and Valocchi, 1990; Dagan, 1991; Rubin, 2003). The top and bottom boundaries will reflect particles back if any attempts to cross it, e.g., effect of local dispersion (such is avoided by choosing an initial location away from the no-flow boundaries).

The time step size is chosen based on the fastest velocity in the solution domain: 10 steps are required to advect a particle outside the fastest-flowing cell. To determine that the effect of overshoot is minimal, particle tracking is repeated for the heterogeneous model by reducing the time step size. This has no discernable effect on the computed particle location. The total time is determined by the approximate time when particles first reach the discharge end, mass is thus conserved for both models. In the heterogeneous model, sub-grid dispersion (which necessarily includes diffusion) is represented by a local longitudinal dispersivity (α_L) of 10^{-3} m and a local transverse dispersivity (α_T) of 10^{-4} m. Given the REV dimensions, these values reflect the magnitude of hydrodynamic dispersion in homogeneous cores (Gelhar et al., 1992; Schulze-Makuch, 2005), or the pore-scale dispersivities (Rubin, 2003). Simulation is also conducted in the heterogenous model by assigning 0.0 local dispersivities. The results are nearly identical to the advective—dispersive case. Thus, for the simulated velocity field and the chosen local dispersivities, local dispersion is negligible.

To evaluate the average tracer behavior, the first two plume central moments are quantified: centroid $(\bar{x}, \bar{z})$ and the plume covariance matrix s_{ij}^2 $(i, j = 1, 2)$. From the initial centroid location, a mean plume displacement (Lp) can be computed. Within the stochastic framework, under the assumptions of stationarity and Fickian transport, components of (ensemble) macrodispersivity are related to the change of (ensemble) s_{ij}^2 over Lp: $\alpha_{ij}^M = \frac{1}{2}\frac{d(s_{ij}^2)}{d(Lp)}$. In this study, however for the single-aquifer experiments, an apparent macrodispersivity is defined

Author's personal copy

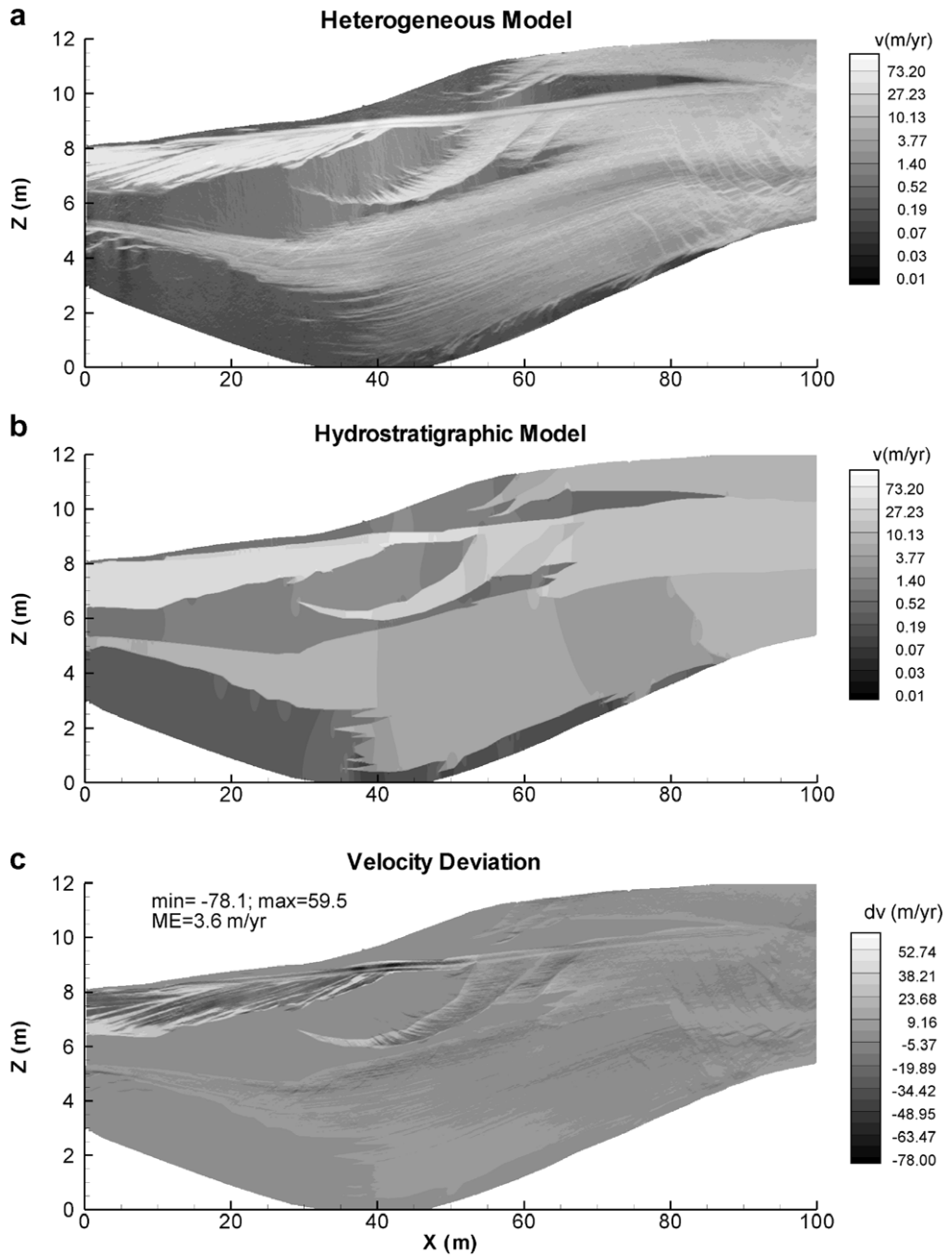

Figure 4 Velocity magnitude of the heterogeneous model (a) and HSM (b), plotted with the same legend. Note that to compare with the lnK map (Fig. 1a), the velocity is plotted in natural log scale. Velocity deviation (Δv) of the HSM (c). A mean error is: $\mathrm{ME} = \frac{1}{n}\sum_{i=1}^{n}|\Delta v|$.

$$\alpha_{ij}^{M} = \frac{1}{2}\frac{s_{ij}^2(t) - s_{ij}^2(0)}{Lp(t) - Lp(0)} \tag{2}$$

where t represents the elapsed time since the tracer is released into the flow field.

The maximum and minimum principal components of α_{ij}^{M} are the longitudinal (α_L^M) and vertical transverse macrodispersivities (α_T^M), respectively. In this study, for the chosen boundary condition, tracer transport occurs laterally, along or at small angles to the bedding plane. Transverse macrodispersion is very limited, e.g., for the heterogeneous simulation (next), an apparent $\alpha_T^M \sim 0.01$ m. This result is consistent with past field observations and stochastic theory predictions. This study evaluates only the longitudinal macrodispersivity.

To evaluate the early and late time behavior, solute breakthroughs are calculated at 4 cross-sections (different displacement distances): $x = 93$ m (w1), $x = 80$ m (w2), $x = 70$ m (w3), $x = 35$ m (w4), each progressively downstream from injection. At each distance, the sampling window is 4 m wide. Over time, the number of particles is counted to represent vertically integrated breakthrough. By comparing the two models, a prediction error is defined as: $\sum_{i=1}^{\mathrm{Ntime}}|N_i^{\mathrm{HSM}} - N_i^{\mathrm{ref}}|/10,000$, Ntime is the number of

Author's personal copy

output times (chosen to ensure a sufficiently smooth breakthrough), N_i^{HSM} and N_i^{ref} is the particle count at ith output predicted by each model.

Tracer simulation in the heterogeneous model

In the heterogeneous model, tracer transport is simulated over 42,048 h (Fig. 5; top panel). The particle trajectories are nearly identical to the groundwater flow paths (not shown). From its initial position, the line source evolves irregularly over time, e.g., at ~10,000 h, the line breaks into three segments, traveling through high-K zones separated by low-K deposits. Moment analysis is used first to evaluate the mass centroid, displacement, and spread from the centroid (Fig. 6; grey curves). Despite the large range of velocities sampled by the particles, the mean displacement over time indicates a near constant plume centroid velocity. The longitudinal covariance (s^2_{max}; the maximum principal covariance) quickly expands until 30,000 h, corresponding to varying lateral tracer displacements from its initial position, as particles enter both faster and slower moving zones. After this time, the covariance decreases slightly for 7000 h, before increasing again. This corresponds to a time a group of fast particles breakthrough the low-K regions at $\sim x < 60$ m. The slow-down, along with the catching-up of the rest of the tracer, results in a slight contraction in the longitudinal direction. This ''negative'' dispersion has a simple physical basis: an appropriate real-world analogy would be a traffic jam. The later covariance expansion corresponds to a time when progressively higher percentages of particles move through the low-K regions. In particular, a group of fastest moving particles enter the turbidite via the connected high-K channels. Overall, due to non-stationarity, the apparent α_L^M does not reach an asymptote. Scale effect is also apparent, i.e., at any time α_L^M is evaluated, it is generally larger than the previous estimate.

During the simulation, particles enter the low-K deposits and are then moved by slow advection: frequently, they enter by advection; other times, they enter by local dispersion. These particles constitute the tail end of the tracer, exhibiting long residence times. (This differs from the class of problems where diffusion dominates in non-flowing, stagnant zones, e.g., LaBolle and Fogg, 2001.) By the end of the simulation, the tracer spreads out laterally over large region of the flow field, exhibited by a leading edge nearly reaching the discharge end while the mass centroid is still lagging behind (the lower portion of the tracer is migrating slowly through the fluvial/floodplain deposit). Accordingly, the breakthrough curves exhibit anomalous behavior (Fig. 7; grey curves). Compared to the ''bell-shaped'' Gaussian profile, longer tails are developed over time, a result of slow-moving particles through the low-K deposits. The shape of the breakthrough is increasingly asymmetrical, as more mass is shifted towards the trailing plume. Comparable to lateral spreading, the breakthrough profile evolves from unimodal to multimodal.

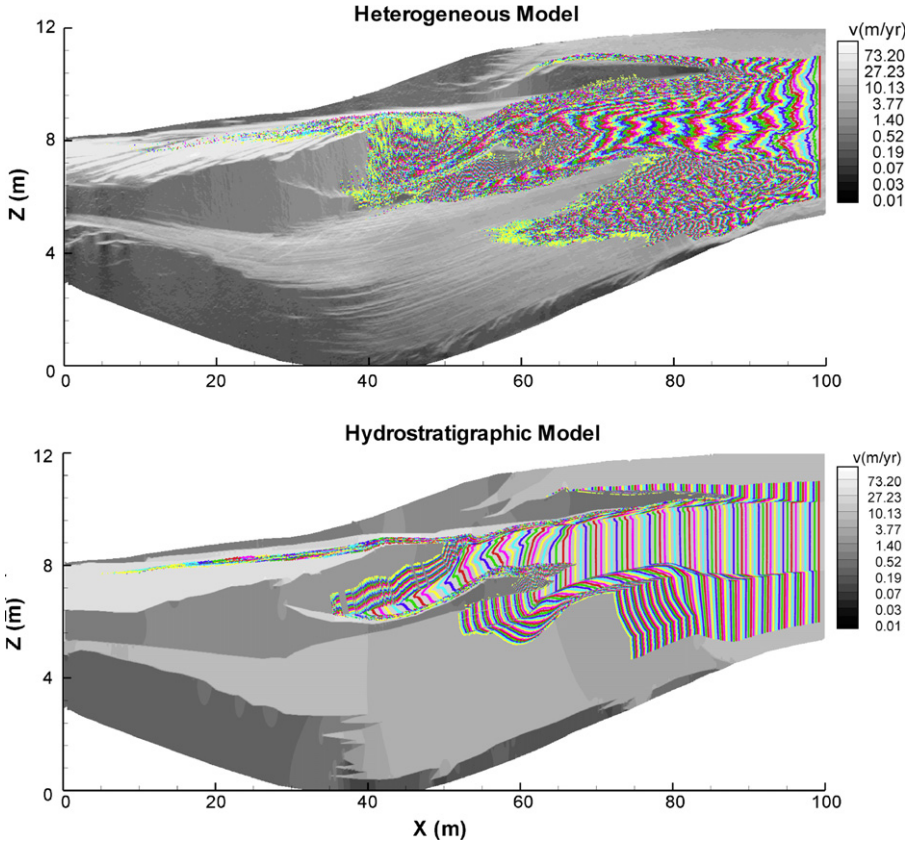

Figure 5 Snapshots of tracer simulated in both models, superimposed onto the respective velocity field. The only difference between models is the velocity field: grid, tracer initialization, time step size, output time, and local dispersivities are the same.

Author's personal copy

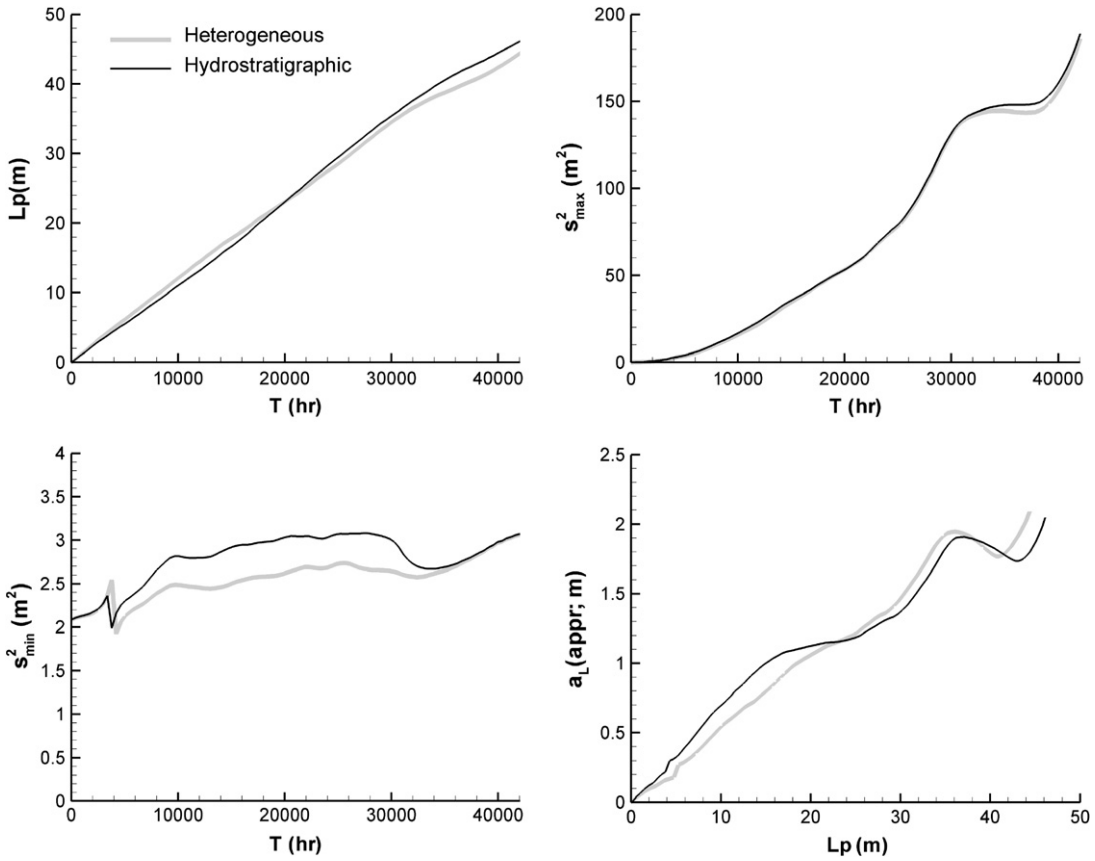

Figure 6 Tracer displacement, longitudinal (s^2_{max}) and transverse covariance (s^2_{min}), and an apparent longitudinal macrodispersivity computed by both models.

Tracer simulations in the HSM

Local dispersion

The same tracer test is repeated in the HSM. Within the smooth velocity field (discretized on the same high-density grid), RWPT is simulated using the same local dispersivities (Fig. 5; lower panel). Such a choice reflects an exploratory analysis where information on heterogeneity is limited, i.e., assuming formation homogeneity. Several observations are made: (1) Compared to the irregular tracer simulated by the heterogeneous model, HSM-predicted tracer is smooth-varying, as expected. (2) Due to the close equivalence in flow paths, both tracers generally travel through the same region of the flow field, reaching similar discharge areas. In later times, the HSM has captured the fast-moving particles through turbidite. (3) Due to the close equivalence in mean (within-unit) velocity and total groundwater flux, HSM-predicted tracer generally corresponds to the mean position of the heterogeneous tracer. However, significant deviation is observed in the trended fluvial-floodplain deposit. (4) Despite the loss of detail in predicting plume shape, the HSM can adequately capture the central moments and the apparent α_L^M (Fig. 6; black curves), suggesting that the average tracer behavior is captured. (5) Anomalous behavior in breakthrough is also predicted (Fig. 7; black curves), e.g., development of long tail and asymmetrical profile, since the largest scale between-unit velocity variations are captured by this model. However, the homogenized within-unit velocity results in breakthroughs of less spread and higher peak concentration, as expected.

Macrodispersion

In the previous simulation using hydrodynamic dispersivities, though tracer moments are closely reproduced, the HSM fails to capture the shape of the breakthrough curves, in particular, the solute arrival time. Since within-unit heterogeneity is non-negligible, the above simulation is repeated using macrodispersivities. Two alternative approaches are used: (a) unit-specific: using an ADE-based stochastic theory, a macrodispersivity is estimated for each unit and mapped to the HSM; (b) time-dependent: macrodispersivity is estimated from moment analysis of the heterogeneous tracer. In the former approach, our aim is not to validate theory (Monte-Carlo simulations are impractical for our large grid). As most units are weakly to moderately heterogeneous, theory is applied in a local sense assuming ergodicity, i.e., assigning an ensemble macrodispersivity to each unit of the HSM. A first-order result from the stochastic literature is used (Dagan, 1988; Rubin, 2003):

$$\begin{aligned} \alpha_L^M(Lp \to \infty) &= \sigma_f^2 \lambda \\ \alpha_T^M(Lp \to \infty) &= 0 \end{aligned} \tag{3}$$

Author's personal copy

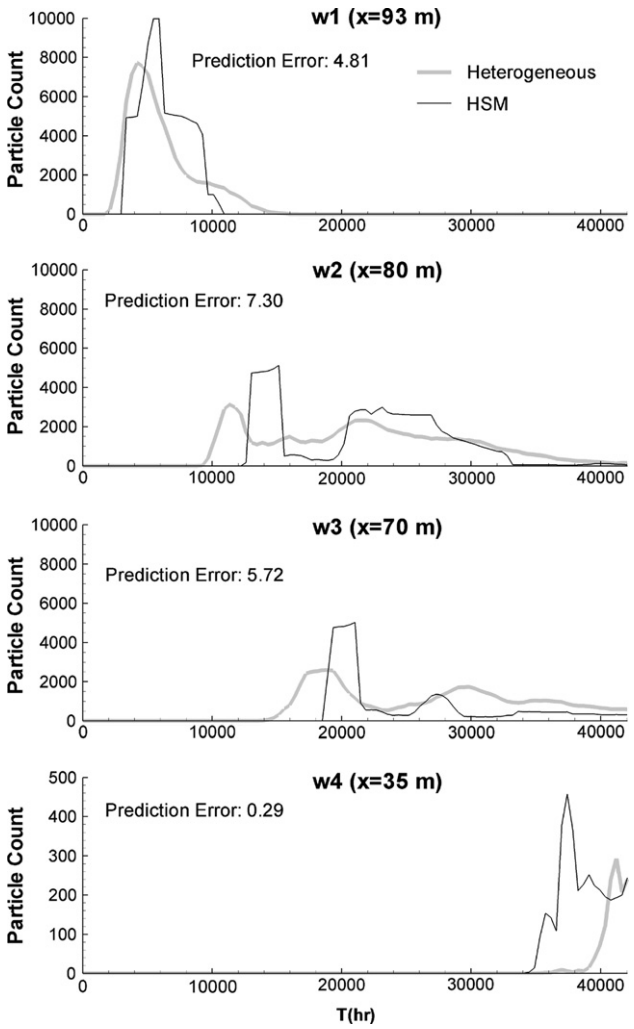

Figure 7 Tracer breakthroughs predicted by both models. A prediction error is shown.

where σ_f^2 is ln*K* variance, λ is ln*K* integral scale along the mean flow direction. This relation applies to two-dimensional (2D) flows in statistically anisotropic media, irrespective of the covariance structure. Specifically, it applies to a large plume, assuming Fickian transport (i.e., large-displacement asymptote), uniform porosity, mean uniform flow, and negligible local dispersion (i.e., the local longitudinal dispersivity is much smaller than λ, which is the case for our chosen α_L). For our conductivity map, however, rigorous adherence to all theory requirements is not possible, e.g., mean uniform flow may only exist in some units. The theory is thus not used in a predictive sense. Rather it provides a suite of first-order (upper-limit) estimates of α_L^M which are then mapped to the units (unit-specific model) (Table 1): α_L^M varies between 0.05 and 0.10 m for the nearly homogenous deepwater units (1, 7, 13, 14) up to 8.06 m for the turbidite. The turbidite unit has the highest ln*K* variance (reflecting the large contrast in sand/clay conductivities) and the longest integral scale along the mean flow direction (reflecting the laterally extensive beds). Both characteristics contribute to the existence of preferential flow paths as exhibited in the heterogenous flow field. α_T^M is assigned 10^{-4} m to all units, representing transverse local dispersion.

Alternatively, a tracer-specific, time-dependent α_L^M is evaluated by fitting a polynomial function to the apparent α_L^M predicted by the heterogeneous model (Fig. 8). Compared to the unit-specific approach which is physical-based, the time-dependent model is phenomenological. However, the time-dependent α_L^M reflects the actual spreading of the tracer for this particular experiment. It increases from 0 to 2.2 m, consistent with the magnitude of theory-predicted α_L^M, suggesting ergodic transport. α_T^M is again assigned 10^{-4} m. Compared to the first approach (α_L^M is evaluated for every particle at every time step depending on which unit it's in), the time-dependent α_L^M is assigned to all particles, regardless of their spatial location.

Results suggest that the macrodispersion models preserve the general position of the heterogeneous tracer (bulk flow is closely captured), but predict a more mixed plume (Fig. 9). At first glance, this may imply the overestimation of macrodispersivity. However, in the heterogeneous model, the fine-scale, within-unit velocity results in a ''zigzagging'' tracer front, thus large lateral expansion. The macrodispersion model, to capture such expansion, results in a large plume relative to the advective case (Fig. 5; lower panel). This behavior is thus implicit to the macrodispersion approach. We speculate that finer stratigraphic division should reduce this effect. When comparing the two macrodispersion models, the unit-specific model predicts upstream dispersion in early times, as α_L^M assigned to units 4, 10, 12 are *asymptotic* values. A small fraction is thus disabled along the recharge boundary (mass loss $\sim$2.9%). The time-dependent model does not suffer this effect: in early times when the *apparent* α_L^M is small, the particles are clustered closer to the heterogeneous tracer. Clearly, theory-predicted values (which are normally reached after large displacements) are less applicable for early time, as expected. In later times, the time-dependent model predicts a larger plume, particularly in turbidite. Overall, however,

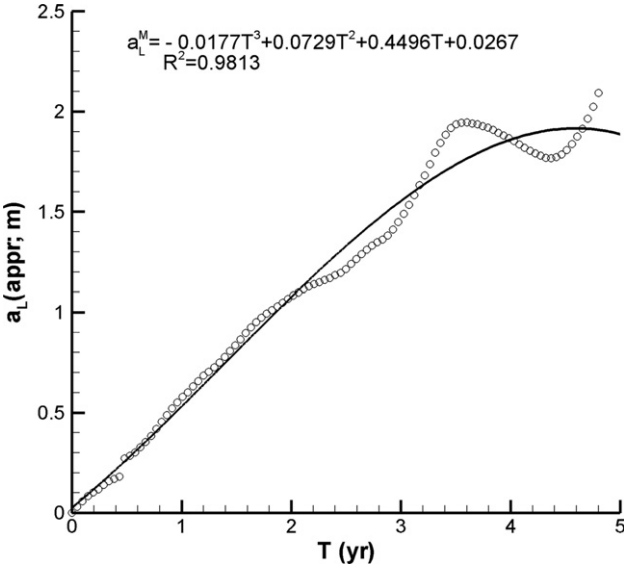

Figure 8 Apparent longitudinal macrodispersivity (circles) of the heterogeneous tracer. A polynomial function is fitted. This is the same macrodispersivity shown in Fig. 6, except *x*-axis is time.

Author's personal copy

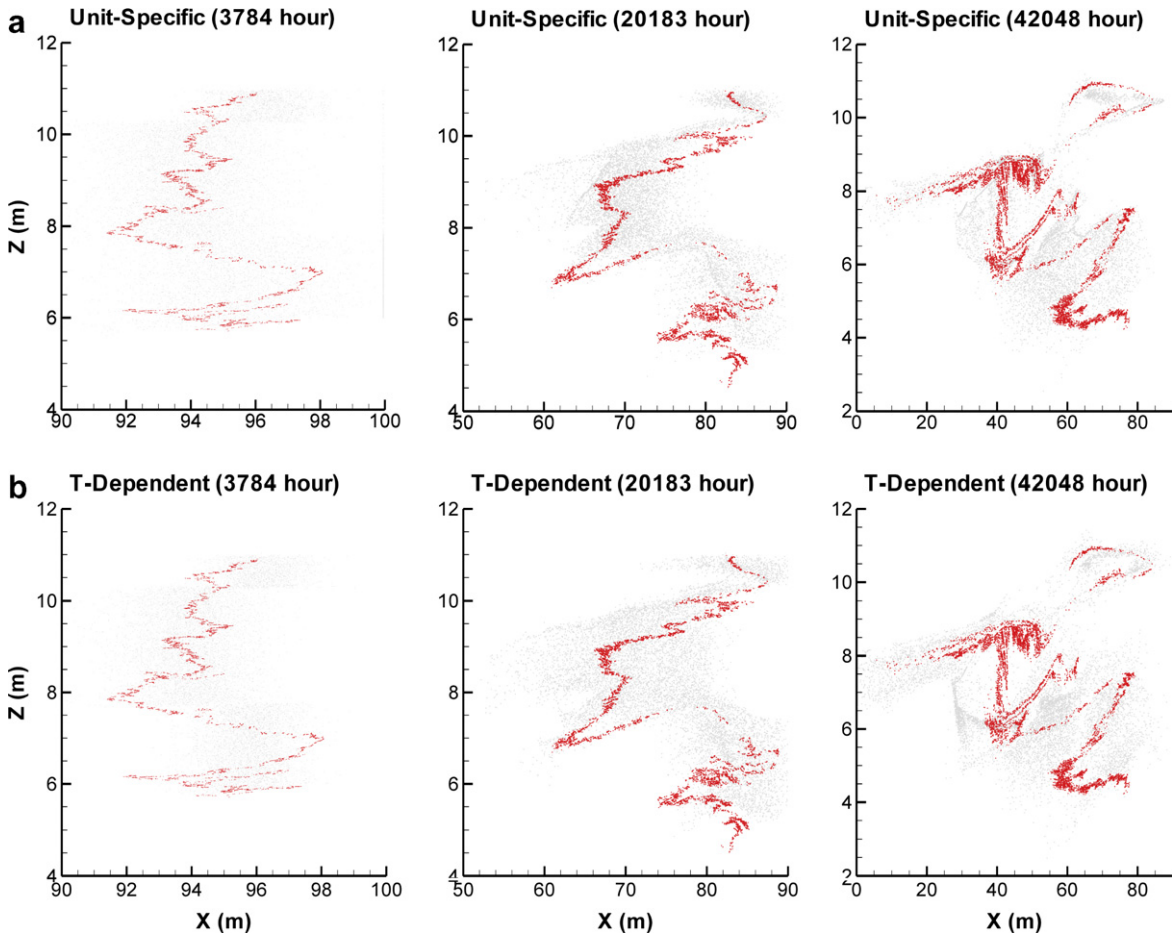

Figure 9 Tracer predicted by the HSM using macrodispersivities (grey): (a) unit-specific; (b) time-dependent. The corresponding location of the heterogeneous tracer (red) is superimposed. For each model, both early, mid and late time predictions are shown. (For interpretation of the references in color in this figure legend, the reader is referred to the web version of this article.)

the differences between the two model predictions are minor, despite the drastically different formulations. This again suggests ergodic transport.

In breakthrough, the use of macrodispersivity results in improved profiles in earlier times (w1–w3) (Fig. 10): compared to the HSM prediction using hydrodynamic dispersivities (Fig. 7), the prediction error is smaller and the timing of early arrival and late tailing more accurate. In particular, while there are significant lags in the solute arrival time when using hydrodynamic dispersivities, such lags no longer exist. Both models further capture the overall asymmetry in breakthrough, as clay-rich units trapping particles for long times. Due to the more mixed plume, they also predict slightly smaller peak concentrations, as was also observed in McLaughlin and Ruan (2001). However, after the solute reaches the turbidite (w4) which exhibits preferential flow paths, both models predict earlier arrivals and higher peak concentrations, indicating the overestimation of macrodispersivity. This finding is not unexpected since channeling of solute in preferential flow paths (as exhibited by the heterogenous model) generally precludes the use of the Fickian-based macrodispersion model (Anderson, 1991). In this case, macrodispersivity is likely not a meaningful parameter. Moreover, throughout simulation time, both models fail to predict the development of a steep front and multiple peak concentrations. Thus, the detailed shape of the breakthrough curve is not well captured by the HSM.

Finally, power-law tails are observed in laboratory and field tracer tests, facilitating parameterization of alternative approaches in modeling transport (e.g., Benson et al., 2000; Haggerty et al., 2000). Compared to ADE, such models can often better predict the tails. The breakthrough curves predicted by all models are re-plotted in the log-log space (Fig. 11). In the heterogenous model, with slight non-linearities, power-law tailing is evident at all locations, suggesting that for the given multiscale heterogeneity, advection-dominated transport can also result in power-law tails. The slope decreases over time, reflecting the development of heavy tail and increasing asymmetry in breakthrough, i.e., more mass is retained in the clay-rich deposits. On the other hand, the macrodispersion models also predict power-law tails. Slightly smaller slopes are observed, e.g., the tail ''concentration'' is overestimated in earlier times (w1) by 10^{1-2} particles. Overall, however, the ADE-based up-scaled model can provide fairly good match. Unlike the non-local approaches, in the case of unit-specific model, no parameter fitting on the observed breakthrough is needed.

and lateral flow BC (resulting in an advection dominated transport regime where solute migration is mostly along stratification, see Fig. 5)

Author's personal copy

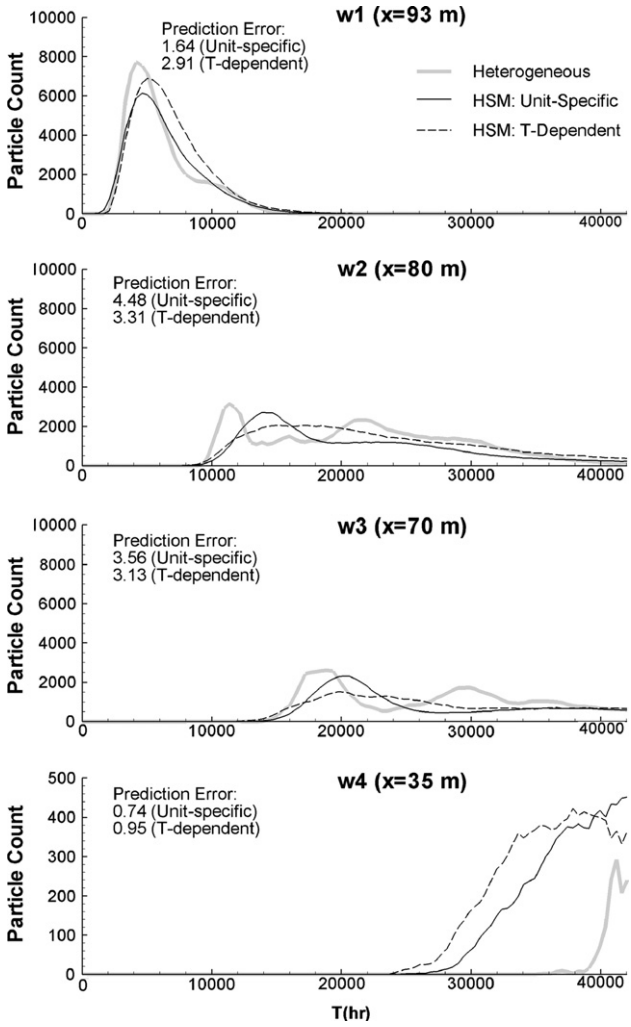

Figure 10 Tracer breakthroughs predicted by the heterogeneous model and the HSM using macrodispersivities. A prediction error is also computed.

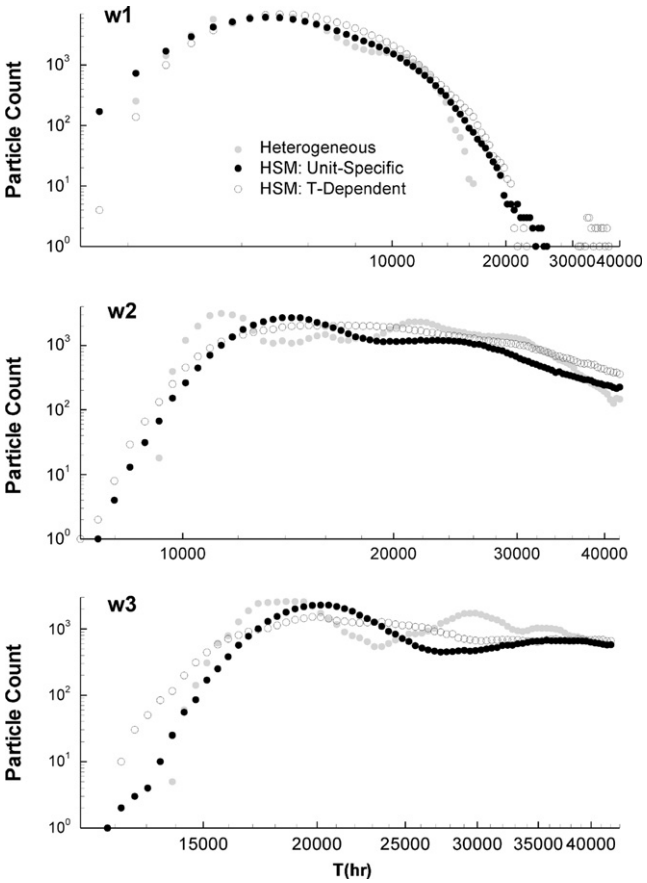

Figure 11 Breakthrough of Fig. 10 in log—log space for w1—w3 (shown for each output time in dots).

Continuous injection

Previous simulations capture solute transport for a tracer released instantly in the upstream flow field. However, real-world contamination in aquifers often persists over time, e.g., solute can dissolve into groundwater and be continuously released from the spill point. To relate to such scenarios, additional simulations are conducted in the heterogenous model and the HSM (using unit-specific macrodispersivities). At the same line-source location, particles are released over time following a normal distribution (Fig. 12). Over a period of 4200 h, a total of 44,704 particles are released into the flow field. The particle locations are again monitored in each model (not shown). At four displacement distances downstream from injection, breakthrough curves are then computed to represent vertically integrated particle mass distribution.

Compared to instant release, considerable smoothing is observed in the breakthroughs of both models due to the effect of plume mixing (Fig. 13). In the heterogeneous model, multimodal breakthrough is again observed which is not predicted by the HSM, though the arrival time is captured well by this model. Similar to instant release, the predicted slope of the HSM breakthrough is smaller. However, unlike instant release, the location of HSM-predicted peak concentration has shifted considerably over time, indicating the importance of source release function on the characteristics of peak breakthrough and its capture by a macrodispersion model. Overall, despite smoothing, the chief strength and weakness of the macrodispersion model persist in similar fashion as in the instant-release scenario. This may be explained by the steady-state flow field in which the continuous transport can be modeled as addition of many instant releases.

Displacement mapping

In this study, the up-scaled transport model is based on ADE, i.e., using macrodispersivities to represent the unresolved, heterogeneity-induced advection. The nature of such advection can be probed by comparing the particle trajectories predicted by the heterogeneous model (using hydrodynamic dispersivities) and the HSM (using zero dispersivities) (Scheibe and Cole, 1994). In each model, 1000 particles are generated uniformly to represent the same instant-release line source (increasing z for increasing particle ID). For the same simulation time, 501 outputs are created at uniform intervals (84.1 h). A macrodispersive displacement vector ($L_x = x_{HSM} - x_{ref}$; $L_z = z_{HSM} - z_{ref}$) is

Author's personal copy

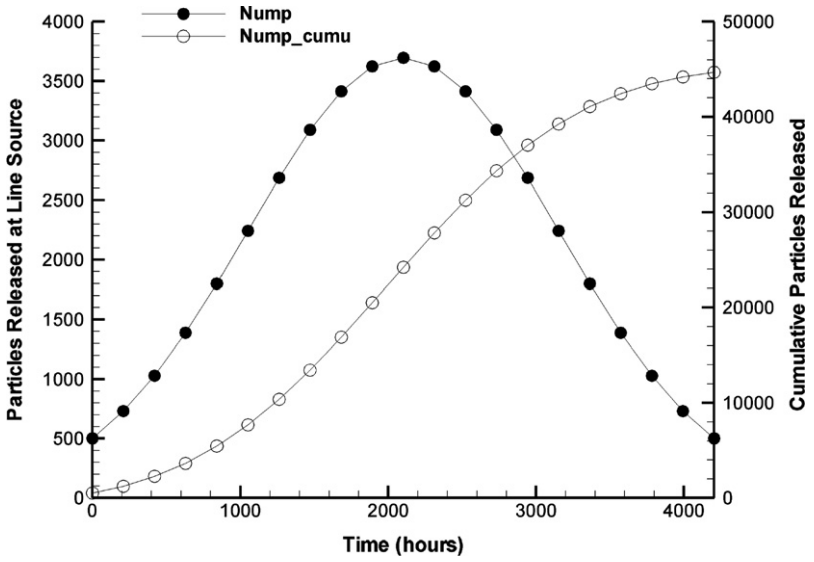

Figure 12 Source release history over time as implemented with random walk. Each dot represents a pulse of particles generated at the same initial line-source location. ''Nump'' is the number of particles released at a given time (left axis); ''Nump-cumu'' is the cumulative number of particles released (right axis).

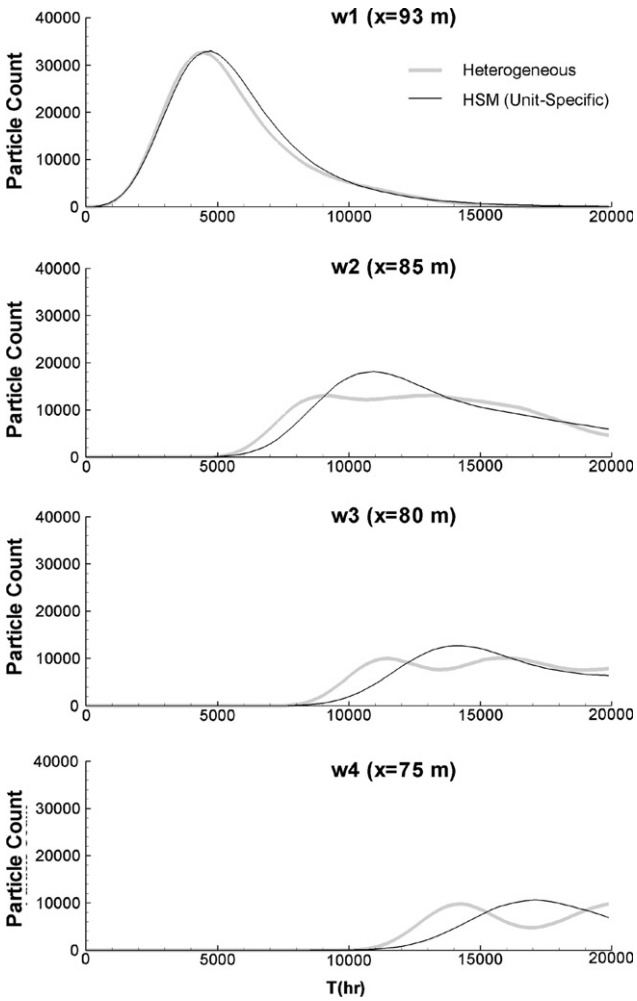

Figure 13 Breakthrough curves predicted by the two models simulating continuous release.

computed for each particle. This vector represents both random processes (sub-REV local dispersion—largely negligible) and deterministic heterogeneity-induced advection. Over time, a surface is created with the output number as *x*-axis, particle ID *y*-axis, and displacement *z*-axis (Fig. 14).

The surface displays dome-like structures, suggesting that the components of the displacement vector are correlated for each particle over time (along ''Output''), as well as among adjacent particles (along ''Particle ID''). This is likely due to the spatially correlated, within-unit velocity field (Fig. 4a). The displacement also grows over time, suggesting increasing deviation from the mean (i.e., up-scaled) flow field. In later times when solute enters the turbidite (large particle ID), the largest deviation is observed in both components. Such correlation, however, is not accounted for by the macrodispersion model: as implemented with RWPT, a ''current'' macrodispersive displacement of a particle is independently generated. The above mapping suggests that such displacement needs to consider the past sequence of displacements over time for which alternative, non-local approaches may be required.

Discussions

Results of this study are discussed in two aspects: (1) the impact of multiscale, non-stationary conductivity heterogeneity on tracer transport; (2) the ability of a hydrostratigraphic model (equivalent conductivity, macrodispersivity) to capture the bulk flow and transport behaviors.

For the chosen boundary condition, the flow field of the heterogeneous model reflects the underlying heterogeneity. In response to changing depositional environment, the velocity is multiscale and non-stationary, resulting in complex tracer behavior throughout space and time. The tracer longitudinal covariance fluctuates, indicating expansion and contraction along the mean flow path. Asymptotic behavior in solute spreading is not observed. By assuming Fickian

Author's personal copy

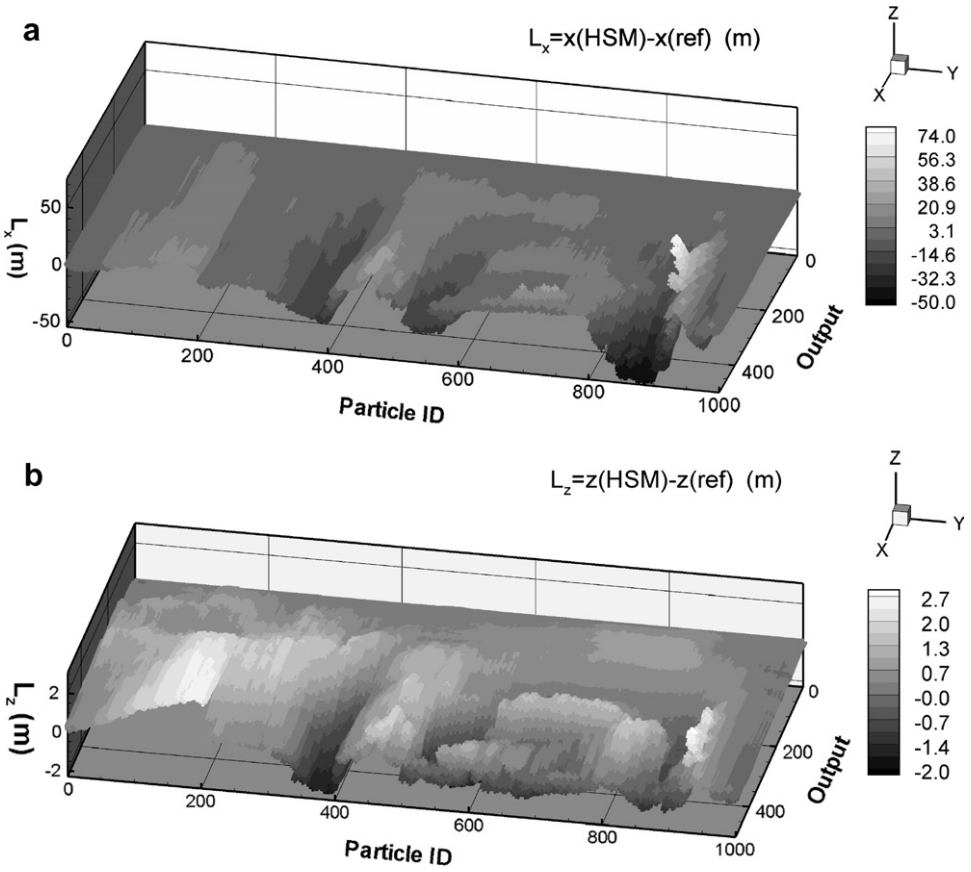

Figure 14 Horizontal (L_x) and vertical (L_z) macrodispersive displacements of each particle over time. Increasing ''Particle ID'' corresponds to increasing initial z value. ''Output'' represents discrete (increasing) output time.

transport, an apparent longitudinal macrodispersivity is found to exhibit ''scale effect''. In this case, it arises due to the imposition of ADE to interpret transport in non-stationary flow. The tracer breakthrough further indicates the development of persistent long tailing associated with anomalous, non-Fickian dispersion.

Flow and transport predictions of the HSM are compared to those of the heterogeneous model. In flow modeling, the HSM closely approximates the hydraulic head, groundwater fluxes, and large-scale between-unit velocity variations. The within-unit velocity predicted by the HSM is smooth, resulting in significant deviation in local velocity. In transport modeling, the HSM using hydrodynamic dispersivities closely predicts the tracer moments and their derivatives, suggesting that dispersivity estimation becomes less important if the average tracer behavior is the goal, i.e., approximate location and extent. However, this model fails to predict the breakthrough arrival, suggesting that the ability of a model to capture the first two moments does not imply sufficiency in predicting higher moments. This is clearly due to the non-Gaussianity of the plume. Overall, large scale between-unit velocity dominates the anomalous behavior and within-unit velocity affects the detailed behavior. For the HSM, despite the close prediction in head and fluxes, detailed tracer behavior is significantly impacted by the unresolved heterogeneity.

When macrodispersivities are used, the overall breakthrough has improved, especially in early times before encountering significant non-stationarity (i.e., turbidite with large σ_f^2). For a large plume, the first-order stochastic theory is able to provide position-dependent estimates that improve breakthrough, especially the solute arrival time. This is despite the fact that theory requirements may not be strictly met within the various units, consistent with the observations made by Desbarats and Srivastava (1991). Both studies suggest that theory can provide realistic parameters for non-stationary media when the deposit is weakly heterogeneous. Moreover, unlike the time-dependent model, model based on theory does not require detailed knowledge on tracer movement, thus is more applicable for field situations when ergodic transport is also satisfied.

In this study, the multiscale conductivity map is represented by the up-scaled model which divides the space into distinct lithofacies units. This approach differs significantly from earlier work when the ADE is evaluated for an undivided domain. For example, at the highly heterogeneous MADE site, the observed dispersivity is $\sim$5 times larger than theory prediction and the macrodispersion model predicts the solute plume poorly (Adams and Gelhar, 1992). Using a single best-fit dispersivity, Liu et al. (2004) concludes that the ADE can not capture the development of asymmetry in breakthrough, even for small σ_f^2. However, within our modeling framework, for variance up to 4.07 (comparable to the MADE site), both macrodispersion models are able to capture the tailing behavior and asymmetry. This suggests that the ADE may be better suited for facies-based modeling. At the MADE

Author's personal copy

site, facies zoning is apparent (see Fig. 2 of Adams and Gelhar, 1992), not unlike the conductivity map of this study. We speculate that the macrodispersion model may improve if the MADE site model is similarly zoned, following the methodology we established herein. The same can be said of the work by Jussel et al. (1994) where the deviation between numerical experiments and theory is attributed to (among others) the existence of distinct sedimentary structures. However, to evaluate the accuracy of any model to match field tests is always hampered by the quality of data characterizing heterogeneity. In this study, the HSM has captured the bulk flow behaviors, precisely because an equivalent conductivity ($\mathbf{K}^*$) is obtained for each unit via up-scaling. In reality, detailed knowledge as required by up-scaling is rarely available. Thus, parallel efforts have been made to evaluate alterative approaches to estimate $\mathbf{K}^*$, again using analytic and stochastic theories (Zhang et al., 2007).

Overall, regardless of the dispersivities, the worst HSM prediction occurs within the trended fluvial/floodplain unit (non-stationarity) and the turbidite unit which contains preferential flows (non-multivariate Gaussian). These are areas requiring more detailed characterization, e.g., finer division. As demonstrated in flow simulations (Zhang et al., 2006), the accuracy of the up-scaled model to predict transport will certainly improve. In particular, finer division will reduce the variability of these units, further satisfying the weak heterogeneity assumption. It must be noted, however, that this study is based on a fixed total variance representative of an unconsolidated deposit. Given the same heterogeneity pattern but with higher variance (e.g., the lower end-member conductivity can be reduced to that of shale), the effect of preferential flow will be accentuated, so will be the degree of breakthrough asymmetry and tailing (Desbarats, 1990; Moreno and Tsang, 1994). This suggests that for higher variances, the performance of the current HSM model will likely degrade. Thus, the level of division will be affected by the level of variability. Based on the experimental stratigraphy, a general modeling methodology is called for to determine the level of characterization that is appropriate for the study objective and variance range.

Finally, this study aims to evaluate the classic (unconditional) macrodispersion model to simulate transport when the small-scale within-unit heterogeneity is not resolved. An experiment-based, synthetic heterogeneity map is used which possesses considerable spatial complexity. The processes simulated are restricted to steady-state flow parallel to bedding and conservative mass transport in this particular 2D map. The insights obtained are thus not expected to be comparable to natural three-dimensional (3D) systems where transient flow effects may be important (e.g., enhanced transverse spreading) (e.g. Bellin et al., 1996). However, the methodology of this study is general and should be applicable to study any spatial dimensions, hydrogeological unit geometry, boundary condition, and heterogeneity style, provided that detailed heterogeneity characterization is available. For example, using consecutive image slices of the experimental deposit, a fully heterogenous 3D model (2,388,015 hexahedral cells) is built with *lagrit* (http://lagrit.lanl.gov/) compiled on a 32-bit linux workstation (larger model is possible in future with 64-bit compilation). This model exhibits multiple sedimentary facies, conductivity non-stationarity, and geostatistical asymmetry (i.e., the integral scale is anisotropic along the horizontal plane). Extending the insights of this study to three-dimensions, it is our belief that as long as the facies-based approach is used with a sufficiently fine division, both the global and within-unit groundwater fluxes can be captured by the HSM, thus tracer centroid trajectory and velocity. However, whether the macrodispersion model can still capture aspects of the higher moments (i.e., breakthrough arrival and tailing) given the additional complexity (i.e., non-axisymmetric anisotropy) remains an open question. This will be addressed in future studies.

Conclusions

A high-resolution fully heterogeneous hydraulic conductivity map provides a basis for evaluating solute transport in a non-stationary medium, and, the impact using a hydrostratigraphic model (HSM) to simulate transport with equivalent conductivity and macrodispersivity. In contrast to numerical aquifers created within a stochastic framework, the process-based map provides a deterministic framework to evaluate transport where local conductivity uncertainties do not exist and heterogeneity is represented to the finest scale. Under a lateral gradient, hydraulic head and groundwater velocity are calculated by both models. A conservative, pulse-input line-source tracer is then simulated. In the heterogeneous model, the tracer exhibits both scale-dependency in the observed longitudinal macrodispersivity and persistent long tailing associated with anomalous, non-Fickian dispersion.

Compared to the predictions of heterogeneous model, the HSM-predicted, global mean relative error of hydraulic head is 1.5%, that of groundwater flux is 0.77%. Using hydrodynamic dispersivities, the HSM closely predicts the evolution of the tracer moments. In breakthrough, a certain degree of tailing is also predicted, as this model captures the largest scale velocity variations between the sand-rich and clay-rich units. However, detailed plume shape is not captured, nor are the arrival and tailing of the breakthrough curves. Using macrodispersivity (both unit-specific and time-dependent), the breakthrough prediction has improved, especially the solute arrival time. Both macrodispersion models also capture the development of breakthrough asymmetry as well as power-law tailing. However, they fail to predict the development of a steep front and multiple peak concentrations. Similar results are also observed for a continuous-source injection. Finally, macrodispersive displacement mapping reveals that heterogeneity-induced dispersion is correlated both in time and space, a likely result of the correlated velocity field.

This study highlights the fact that for the given boundary condition and plume source dimensions, the up-scaled model based on ADE can capture certain key aspects of the bulk (steady-state) flow and transport behaviors in a non-stationary medium with realistic heterogeneity pattern and variance range. By using space- or time-varying dispersivities, important transport characteristics such as solute arrival and tailing can be captured (further improvement is possible with more refined lithofacies division). This study also highlights the fact that the accuracy of transport prediction hinges on the accuracy of flow modeling. For multiscale media, it is thus critical to first develop a correct framework

Author's personal copy

for flow modeling. The flexible, lithofacies-based approach is a natural choice for such modeling. However, since a deterministic flow/transport framework is adopted in this study (i.e., perfect knowledge of heterogeneity down to the smallest resolvable scale; perfect knowledge of the lithofacies boundaries), we do not attempt to address the issue of formulating and quantifying flow/transport uncertainties due to imperfect knowledge. Recent developments that do address this issue in multiscale media within the stochastic framework are reviewed by Winter et al. (2003).

To summarize, compared to many studies that evaluate flow and transport at two scales, this study has several unique aspects: (1) the heterogeneous model is created from a process-based map; the up-scaled model is based on geological facies division. (2) a high-density grid is used by all models of flow and transport, eliminating uncertainties due to grid coarsening. (3) the conductivity up-scaling is flexible and applicable to irregular-shaped deposits (depending on heterogeneity, $\mathbf{K}^*$ can be scalar or fully tensorial). (4) parameters for the up-scaled model ($\mathbf{K}^*$; unit-specific macrodispersivity) are obtained via forward approaches, i.e., no calibration is used to fit the results to those of fine-scale simulations. Future work will explore (1) the conditional macrodispersion model on improving the current unconditional predictions; (2) other heterogeneity maps (e.g., 2D detailed outcrop mapping) and 3D systems; (3) Against high-resolution simulations, alternative transport modeling approaches may be evaluated.

In this study, given the large grid size of the flow and transport experiments, the computational challenge deserves special mention. The 2D flow and transport experiments were able to use serial codes running on a 64-bit IBM supercomputer. Using Gaussian Elimination, the flow simulation was completed within $\sim$3 h; a later re-run of the code utilizing an iterative solver gave the same results in less than a hour. The particle tracking simulations were able to finish in $\sim$2 days. However, the computation requirement of the 3D model will be much higher. As part of the ongoing research, a parallel 3D groundwater flow code calling the MPI and PETSc (Balay et al., 2001) libraries has been written and validated against both analytic predictions and numerical results (a separate serial code was written to provide verification). A parallel random walk particle tracking code will also be developed. Extending the facies mapping approach of the 2D studies, a new mapping scheme is currently being developed which will allow the delineation of irregular facies units in three-dimensions.

Acknowledgements

The work is supported by the Turner Postdoc Fellowship of the Department of Geological Sciences, University of Michigan. Ye Zhang acknowledges the use of an IBM Libra supercomputer at the Indiana University.

References

Adams, E.E., Gelhar, L.W., 1992. Field study of dispersion in a heterogenous aquifer 2. spatial moments analysis. Water Resources Research 28, 3293–3307.

Anderson, M.P., 1991. Comment on ''universal scaling of hydraulic conductivities and dispersivities in geologic media'' by S. P. Neuman. Water Resources Research 27, 1381–1382.

Anderson, M.P., 1997. Characterization of geological heterogeneity. In: Subsurface flow and transport: a stochastic approach. Cambridge University Press, pp. 23–43.

Balay, S., Buschelman, K., Gropp, W.D., Kaushik, D., Knepley, M.G., McInnes, L.C., Smith, B.F., Zhang, H., 2001. PETSc Web page, <http://www.mcs.anl.gov/petsc>.

Bellin, A., Dagan, G., Rubin, Y., 1996. The impact of head gradient transients on transport in heterogeneous formations: Application to the borden site. Water Resources Research 32, 2705–2713.

Benson, D.A., Wheatcraft, S.W., Meerschaert, M.M., 2000. Application of a fractional advection–dispersion equation. Water Resources Research 36, 1403–1412. doi:10.1029/2000WR90-0031.

Berkowitz, B., Klafter, J., Metzler, R., Scher, H., 2002. Physical pictures of transport in heterogeneous media: advection–dispersion, random walk and fractional derivative formulations. Water Resources Research 38, 1191. doi:10.1029/2001WRR00-1030.

Bersezio, R., Bini, A., Giudici, M., 1999. Effects of sedimentary heterogeneity on groundwater flow in a quaternary pro-glacial delta environment: joining facies analysis and numerical modeling. Sedimentary Geology 129, 327–344.

Cortis, A., Gallo, C., Scher, H., Berkowitz, B., 2004. Numerical simulation of non-fickian transport in geological formations with multiple-scale heterogeneities. Water Resources Research 40. doi:10.1029/2003WR002750.

Cushman, J.H., Ginn, T.R., 1993. Non-local dispersion in media with continously evolving scales of heterogeneity. Transport in Porous Media 13, 123–138.

Dagan, G., 1988. Time-dependent macrodispersion for solute transport in anisotropic heterogeneous aquifers. Water Resources Research 24, 1491–1500.

Dagan, G., 1989. Flow and Transport in Porous Formations. Springer-Verlag.

Dagan, G., 1991. Dispersion of a passive solute in non-ergodic transport by steady velocity fields in heterogeneous formations. Journal of Fluid Mechanics 233, 197–210.

Dagan, G., Neuman, S.P., 1997. Subsurface Flow and Transport: A stochastic appraoch. Cambridge University Press, New York.

Desbarats, A.J., 1990. Macrodispersion in sand-shale sequences. Water Resources Research 26, 153–163.

Desbarats, A.J., Srivastava, R.M., 1991. Geostatistical characterization of groundwater flow parameters in a simulated aquifer. Water Resources Research 27, 687–698.

Efendiev, Y., Durlofsky, L.J., Lee, S.H., 2000. Modeling of subgrid effects in coarse-scale simulations of transport in heterogeneous porous media. Water Resources Research 36, 2031–3041.

Eggleston, J., Rojstaczer, S., 1998. Identification of large-scale hydraulic conductivity trends and the influence of trends on contaminant transport. Water Resources Research 34, 2155–2168.

Feehley, C.E., Zheng, C., Molz, F.J., 2000. A dual-domain mass transfer approach for modeling solute transport in heterogeneous aquifers: application to the macrodispersion experiment (MADE) site. Water Resources Research 36, 2501–2515.

Fernàndez-Garcia, D., Gómez-Hernández, J.J., 2007. Impact of upscaling on solute transport: traveltimes, scale dependence of dispersivity, and propagation of uncertainty. Water Resources Research 43. doi:10.1029/2005WR004727.

Fogg, G.E., 1990. Architecture and Interconnectedness of Geologic Media: Role of the Low-permeability Facies in Flow and Transport. Verlag Heinz Heise, Hannover, Germany, pp. 19–40.

Gelhar, L., 1993. Stochastic Subsurface Hydrology. Prentice Hall.

Author's personal copy

Gelhar, L.W., Welty, C., Rehfeldt, K., 1992. A critical review of data on field-scale dispersion in aquifers. Water Resources Research 28, 1955–1974.

Glimm, J., Lindquist, W.B., Pereira, F., Zhang, Q., 1993. A theory of macrodispersion of the scale-up problem. Transport in Porous Media 13, 97–122.

Guadagnini, A., Neuman, S.P., 2001. Recursive conditional moment equations for advective transport in randomly heterogeneous velocity fields. Transport in Porous Media 42, 37–67.

Haggerty, R., Gorelick, S.M., 1995. Multiple-rate mass transfer for modeling diffusion and surface reactions in media with pore-scale heterogeneity. Water Resour. Res. 31, 2383–2400. doi:10.1029/95WR01583.

Haggerty, R., McKenna, S.A., Meigs, L.C., 2000. On the late-time behavior of tracer test breakthrough curves. Water Resources Research 36, 3467–3479.

Harvey, C., Gorelick, S., 2000. Rate-limited mass transfer or macrodispersion: Which dominates plume evolution at the macrodispersion experiment (MADE) site? Water Resources Research 36.

Hoeksema, R.J., Kitanidis, P.K., 1985. Analysis of the spatial structure of properties of selected aquifers. Water Resources Research 21, 563–572.

Jussel, P., Stauffer, F., Dracos, T., 1994. Transport modeling in heterogenous aquifers: 2. three-dimensional transport model and stochastic numerical tracer experiments. Water Resources Research 30, 1819–1832.

LaBolle, E.M., Fogg, G.E., 2001. Role of molecular diffusion in contaminant migration and recovery in an alluvial aquifer system. Transport in Porous Media 42, 155–179.

LaBolle, E.M., Fogg, G.E., Tompson, A.F.B., 1996. Random-walk simulation of transport in heterogeneous porous media: Local mass-conservation problem and implementation methods. Water Resources Research 32, 583–594. doi:10.1029/95WR03528.

Liu, G., Zheng, C., Gorelick, S.M., 2004. Limits of applicability of the advection–dispersion model in aquifers containing connected high-conductivity channels. Water Resources Research 40. doi:10.1029/2003WR002735.

Lu, S., Molz, F., Fogg, G., Castle, J.W., 2002. Combining stochastic facies and fractal models for representing natural heterogeneity. Hydrogeology Journal 10, 475–482.

McLaughlin, D., Ruan, F., 2001. Macrodispersivity and large-scale hydrogeologic variability. Transport in Porous Media 42, 133–154.

Morales-Casique, E., Neuman, S.P., Guadagnini, A., 2006. Non-local and localized analyses of non-reactive solute transport in bounded randomly heterogeneous porous media: Theoretical framework. Advances in Water Resources 29, 1238–1255.

Moreno, L., Tsang, C.-F., 1994. Flow channeling in strongly heterogeneous porous media: A numerical study. Water Resources Research 30, 1421–1430.

Neuman, S.P., 1997. Stochastic approach to subsurface flow and transport: A view to the future. In: Subsurface Flow and Transport a Stochastic Approach. Cambridge University Press, pp. 231–241.

Quinodoz, H., Valocchi, A., 1990. Macrodispersion in heterogeneous aquifers: numerical experiments. In: Moltyaner, G. (Ed.), Transport and Mass Exchange Processes in Sand and Gravel Aquifers: Field and Modeling Studies. Atomic Energy Canada, pp. 465–468.

Renard, P., de Marsily, G., 1997. Calculating equivalent permeability: a review. Advances in Water Resources 20, 253–278.

Rubin, Y., 2003. Applied Stochastic Hydrogeology. Oxford University Press.

Rubin, Y., Bellin, A., Lawrence, A.E., 2003. On the use of block-effective macrodispersion for numerical simulations of transport in heterogeneous formations. Water Resources Research 39. doi:10.1029/2002WR001727.

Sanchez-Vila, X., Guadagnini, A., Carrera, J., 2006. Representative hydraulic conductivities in saturated groundwater flow. Reviews of Geophysics, 44, paper number 2005RG000169.

Scheibe, T.D., Cole, C.R., 1994. Non-Gaussian particle tracking: application to scaling of transport processes in heterogeneous porous media. Water Resources Research 30, 2027–2039.

Scheibe, D.T., Freyberg, D.L., 1995. Use of sedimentological information for geometric simulation of natural porous media structure. Water Resources Research 31, 3259–3270.

Schulze-Makuch, D., 2005. Longitudinal dispersivity data and implications for scaling behavior. Ground Water 43, 443–456.

Tompson, A.F.B., Falgout, R.D., Smith, S.G., Bosl, W.J., Ashby, S.F., 1998. Analysis of subsurface contaminant migration and remediation using high performance computing. Advances in Water Resources 22, 203–221.

Webb, E.K., Anderson, M.P., 1996. Simulation of preferential flow in three-dimensional, heterogeneous conductivity fields with realistic internal architecture. Water Resources Research 32, 533–545.

Webb, E.K., Davis, J.M., 1998. Simulation of the Spatial Heterogeneity of Geologic Properties, An Overview. SEPM (Society for Sedimentary Geology), Tulsa, OK, United States.

Weissmann, G.S., Zhang, Y., LaBolle, E.M., Fogg, G.E., 2002. Dispersion of groundwater age in an alluvial aquifer system. Water Resources Research 38, 1198. doi:10.1029/2001WR000907.

Wheatcraft, S.W., Cushman, J.H., 1991. Hierarchical approaches to transport in heterogeneous porous media, Reviews of Geophysics Supplement, pp. 263–269.

Winter, C.L., Tartakovsky, D.M., Guadagnini, A., 2003. Moment differential equations for flow in highly heterogeneous porous media. Surveys in Geophysics 24, 81–106.

Zhang, Q., 1992. A multi-length-scale theory of the anomalous mixing-length growth for tracer flow in heterogenous porous media. Journal of Statistical Physics 66, 485–501.

Zhang, Y., 2005. Determination of effective hydrological parameters using experimental stratigraphy, Ph.D. thesis, Indiana University.

Zhang, Y.-K., Neuman, S.P., 1990. A quasi-linear theory of non-fickian and fickian subsurface dispersion, 2. application to anisotropic media and the borden site. Water Resources Research 26, 903–913.

Zhang, Y., Person, M., Merino, E., Szpackiwcz, M., 2005a. Evaluation of soluble benzene migration in the Uinta basin. Geofluids 5, 106–123.

Zhang, Y., Person, M., Paola, C., Gable, C., Wen, X.-H., Davis, J., 2005b. Geostatistical analysis of an experimental stratigraphy. Water Resources Research 41. doi:10.1029/2004WR003756.

Zhang, Y., Gable, C.W., Person, M., 2006. Equivalent hydraulic conductivity of an experimental stratigraphy – implications for basin-scale flow simulations. Water Resources Research 42, w05404. doi:10.1029/2005WR004720.

Zhang, Y., Person, M., Gable, C.W., 2007. Representative hydraulic conductivity of hydrogeologic units: Insights from an experimental stratigraphy. Journal of Hydrology 339, 65–78. doi:10.1016/ j.jhydrol.2007.03.007.

Zhou, Q., Liu, H., Bodvarsson, G.S., Oldenburg, C.M., 2003. Flow and transport in unsaturated fractured rock: effects of multi-scale heterogeneity of hydrogeologic properties. Journal of contaminant hydrology 60, 1–30.